

Analysis on the structural variation during the stretching and recovery of Elastomeric Fibers prepared from Polypropylenes of Low Stereo-regularity

T. Sakurai^a, W. Takarada^a, T. Kikutani^{a*}, T. Takebe^b, Y. Minami^b, Y. Kohri^b, T. Kanai^b,
L. Rong^c, S. Toki^c, B. S. Hsiao^c

^aDepartment of Organic and Polymeric Materials, Graduate School of Science and Engineering,
Tokyo Institute of Technology, O-okayama, Meguro-ku, Tokyo 152-8552, Japan

^bPerformance Materials Laboratories, Idemitsu Kosan Co., Ltd.,
Anesaki-Kiagan, Ichihara, Chiba 299-0193, Japan

^cDepartment of Chemistry, Stony Brook University, Stony Brook, New York 11794-3400, USA

*Corresponding author: kikutani.t.aa@m.titech.ac.jp

Abstract. Polypropylene (PP) with controlled low stereo-regularity (L-PP) have been attracting considerable attention as a new type of thermoplastic elastomer. In this study, three types of PPs, *i.e.* L-PP, L-PP blended with 15 wt% of high stereo-regularity/low molecular weight PP (L-PP-LMC) and L-PP blended with 15 wt% of high stereo-regularity/high molecular weight PP (L-PP-HMC) were prepared. High-speed melt spinning of these polymers were conducted at various take-up velocities to obtain fibers with wide variety of elastomeric properties. There was a considerable improvement of processability by the blending of high stereo-regularity PP. Tensile test during stretching and recovery revealed that elastic recovery took a maximum value at a relatively low take-up velocity, whereas the blending of high stereo-regularity PP leads to the increase of tensile modulus and slight reduction of elastic recovery. In-situ WAXD and SAXS measurements were carried out during the tensile test. Good recoverability of higher-order structure after the stretching and recovery, which was characterized by the reduction of the amount of a*-axis oriented crystals and decrease of the orientation of c-axis oriented crystals during stretching, was found to be the characteristics of fibers with good elastic recoverability.

Introduction

Development of metallocene catalysts enabled us to control the molecular weight distribution and composition distribution of polypropylenes (PP), which may lead to the improved controllability of the higher order structure and properties of end-products [1-3]. Particularly, low stereo-regularity PP (L-PP) prepared with such technology is expected to be applied for the production of elastomeric nonwoven fabrics through the spunbonding process. Because L-PP essentially has low crystallization rate, however, the delayed solidification could cause troubles during the fiber formation processes. Considering the above, effect of the blending of high stereo-regularity PP into L-PP on the processability in the high-speed melt spinning process and the mechanical properties of resultant fibers was investigated in this study. As elastic recovery after stretching is one of the most important characteristics of the elastomeric fibers,

recoverability of the prepared fibers were analyzed by the tensile testing. Along with this experiment, structural change of the fibers during the stretching and recovery were analyzed by in-situ wide-angle and small-angle X-ray scattering measurement utilizing the strong X-ray source of a synchrotron radiation facility.

Experimental

Material

Three types of PP, *i.e.* low stereo-regularity PP (L-PP), LMPP blended with 15 wt% of high stereo-regularity/low molecular weight PP (L-PP-LMC) and LMPP blended with 15 wt% of high stereo-regularity/high molecular weight PP (L-PP-HMC) were prepared for the melt spinning. Characteristics of the three types of polymer for blending are summarized in Table 1. Molecular weights of L-PP and LMC were similar.

Table 1. Characteristics of polymers for blending

Polymer code	MFR (g/10 min)	Melting Temp.
L-PP	60	59.6 °C
LMC	60	160.4 °C
HMC	20	161.0 °C

Melt spinning

High-speed melt spinning process was applied for the formation of fibers from three types of PPs. i.e. L-PP, L-PP-LMC and L-PP-HMC. Polymers were melted at 210 °C and extruded through a spinning nozzle of 0.6 mm diameter at the throughput rate of 2.0 g/min. Take-up velocity was varied from 0.3 km/min to the attainable highest velocity. In the melt spinning process, on-line measurement of the fiber diameter was carried out at various positions to analyze the thinning behavior of fibers along the spinning line.

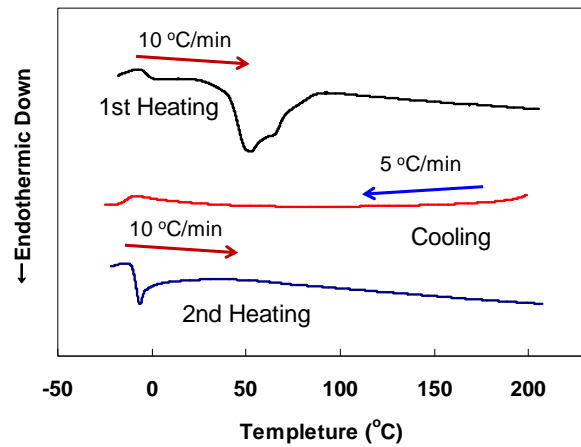
Characterization of fibers

Tensile tests and elastomeric recovery measurements were conducted to analyze the mechanical properties of prepared fibers. Differential scanning calorimetry (DSC), thermo-mechanical analysis (TMA), and Wide-angle X-ray Diffraction (WAXD) measurements at elevated temperatures were carried out to analyze the thermal property of fibers. In addition, structural changes during the stretching and recovery of prepared fibers were investigated through the in-situ measurements of WAXD and Small-angle X-ray Scattering (SAXS) patterns utilizing X27C beam line at the National Synchrotron Light Source in New York, USA.

Results and Discussion

Material characterization

DSC diagram of L-PP measured during the 1st heating, cooling and 2nd cooling processes are shown in Fig. 1. In the 1st heating process, endothermic peak of melting was observed at around 50 °C. In the cooling process, no crystallization peak was observed even though slow cooling rate of 5 °C/min was adopted. When the 2nd heating was applied immediately after the cooling down to around -20 °C, only the glass transition was observed. Extremely low crystallizability of LMPP was confirmed through this analysis.

**Fig.1** DSC thermograms of L-PP pellet measured during 1st heating, cooling and 2nd heating processes.

Spinning behavior

The attainable highest take-up velocities of L-PP, L-PP-LMC, and L-PP-HMC were 6, 7, and 10 km/min, respectively. This result means that the spinnability of L-PP was improved by the blending of high-stereo-regularity PP. It should be noted that the L-PP fibers could not be prepared at take-up velocities lower than 1 km/min because the multiple fibers stuck each other on the take-up bobbin. This result indicated that the fibers were still in an amorphous state when they moved along the spinning line and reached to the bobbin. This is due to the low crystallizability of L-PP. On the other hand, the L-PP-LMC and L-PP-HMC fibers were separated each other on the bobbin at all the take-up velocities investigated. In other words, processability was improved by the blending of high-stereo-regularity PP. Another interesting feature is that the L-PP fibers were separated each other at higher take-up velocities. This result is attributable to the enhancement of crystallization caused by tensile stress applied in the spinning line.

Results of on-line fiber diameter measurement are shown in Fig. 2. So called “neck-like deformation” was observed at high take-up velocities for the three types of polymers. L-PP and L-PP-LMC showed similar thinning behavior, whereas the position of neck-like deformation shifted to upper stream in L-PP-HMC. Higher viscosity of HMC because of its high molecular weight was

considered to be the origin of this behavior because enhanced viscoelastic effect and/or enhancement of stress-induced crystallization were expected to occur. It should be noted that additional thinning of spinning line was clearly observed after the neck-like deformation. In this region elastic deformation of fiber was occurring because of the extremely low tensile modulus of running fibers.

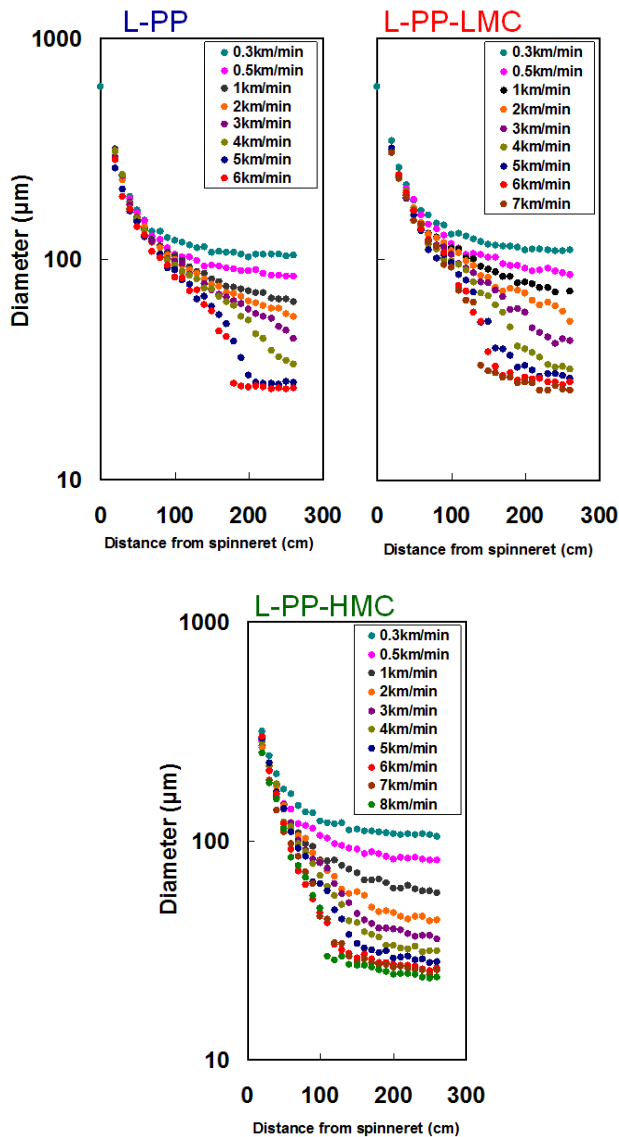


Fig.2 Thinning behaviors of fiber diameter along the spinning line for three types of PP melt-spun at different take-up velocities.

Mechanical properties of fibers

Tensile test of prepared fibers revealed the tendency of higher tenacity and lower elongation at break by the blending of high stereo-regularity PP. Variations of tensile modulus of prepared fibers with take-up velocity for the three types of PP are shown in Fig. 3. Tensile modulus of L-PP remained at low values of less than 50 MPa at all the take-up velocities. Blending of high stereo-regularity PP caused the increase of tensile modulus especially at high take-up velocities. This effect was more significant when high stereo-regularity/high molecular weight PP was blended into LMPP. It should be noted that the maximum tensile modulus of around 500 MPa for L-PP-HMC is still much lower than the tensile modulus of ordinary PP fibers prepared from high-stereo regularity PP, i.e. around 2 – 4 GPa.

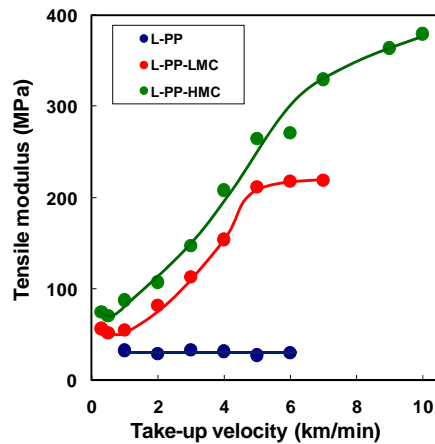


Fig.3 Variation of tensile modulus with take-up velocity for fibers prepared from three different PPs.

Elastic recovery of fibers after 100 % extension is shown in Fig. 4. In the first cycle, elastic recovery took a maximum value at a relatively low take-up velocity, whereas the blending of high stereo-regularity PP leads to the slight reduction of elastic recovery. On the other hand, recovery from the second cycle extension was higher than that from the first cycle extension, and showed high recovery of about 95 % for all the samples

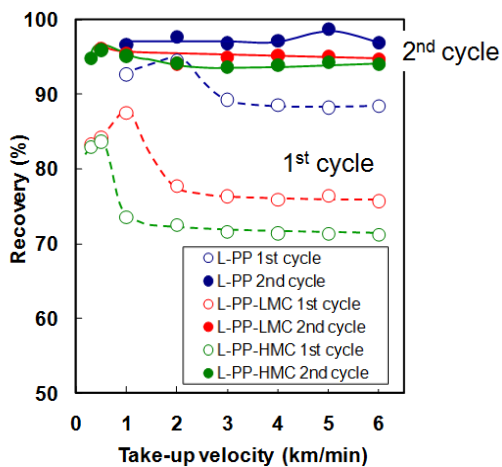


Fig.4 Variations of recovery with take-up velocity for fibers prepared from three different PPs. First and second cycle measurements were performed applying 100% extension.

Thermal properties

For the L-PP and L-PP-LMC fibers prepared at 5 km/min, variation of WAXD patterns with the increase of temperature was measured. WAXD patterns obtained at 30, 50, 70 and 100 °C are shown in Fig. 5. The structure with highly oriented monoclinic crystals was found for the as-spun fibers of both polymers. When the temperature was elevated to 70 °C, crystals in L-PP fibers started to melt, whereas crystalline diffraction of the L-PP-LMC fibers remained intact. At 100 °C, crystalline orientation of L-PP-LMC fibers decreased slightly, whereas disappearance of crystalline diffractions was confirmed for the L-PP fibers.

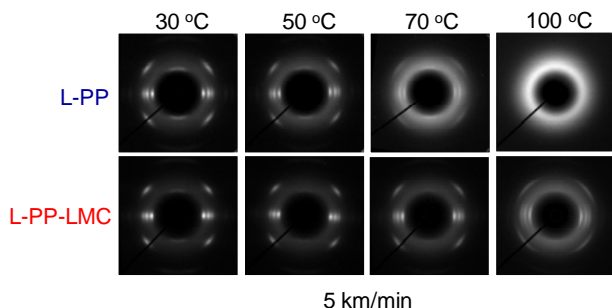


Fig.5 Changes of WAXD pattern with increasing temperature for L-PP and L-PP-LMC fibers obtained at 5 km/min.

Result of TMA measurement is shown in Fig. 6. Shrinkage stress showed higher maximum value and remained up to around 200 °C for the fibers prepared from L-PP-LMC and L-PP-HMC. This result is in accordance with the result shown in Fig. 5. In other words, heat resistance of L-PP fibers, which has extremely low melting point, was significantly improved by the blending of high stereo-regularity PP.

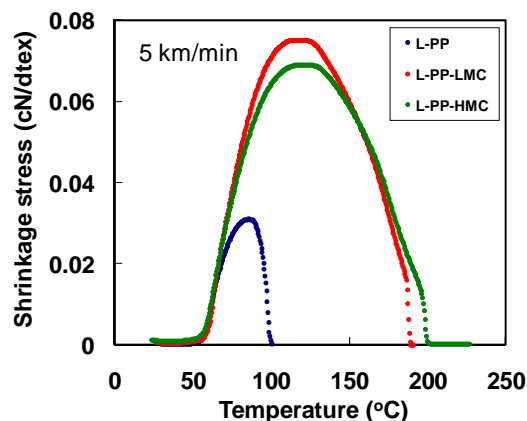


Fig.6 Shrinkage stress versus temperature curves of fibers of three different PPs prepared at 5 km/min.

Structural change during stretch and recovery

Results of in-situ WAXD and SAXS measurement during stretch and recovery of L-PP fibers obtained at take-up velocities of 1, 2 and 5 km/min are shown in Figs. 7, 8 and 9, respectively. It should be noted that the fiber obtained at 2 km/min showed the highest recoverability after stretching as shown in Fig.4.

As can be seen in Fig.7, the WAXD pattern of as-spun fiber (0% strain) obtained at 1 km/min was consisting of monoclinic (α -form) crystals. Degree of crystalline orientation was very low, however there was a slight indication of the co-existence of the crystals of c-axis and a*-axis orientations. When fiber was stretched to 94 %, the WAXD pattern revealed the drastic structural change to the highly oriented monoclinic crystals with the orientation of c-axis along the fiber axis. When length of the fiber was recovered to 19% stretch, monoclinic crystals with mild orientation remained

in the structure. The SAXS pattern of as-spun fiber showed a circular pattern with the concentration of intensity at the meridian. At the 94 % stretch, SAXS pattern changed to the x-shaped pattern, and after the recovery to 19%, the SAXS pattern almost returned to that of as-spun fibers.

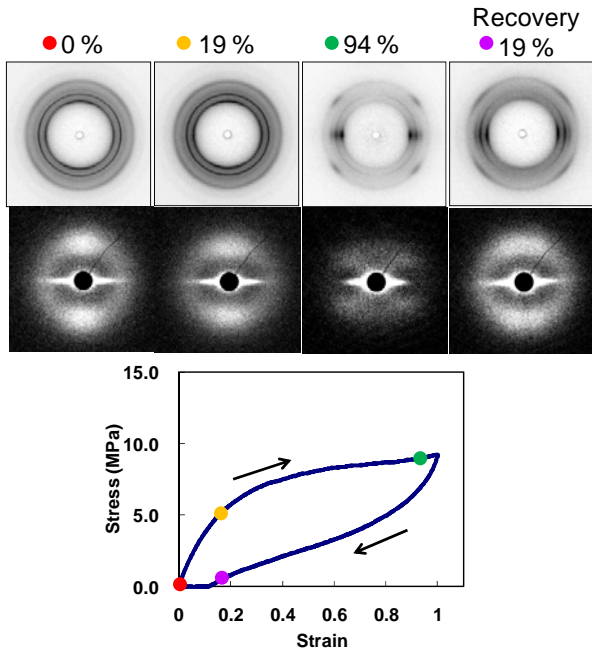


Fig.7 Changes of WAXD and SAXS patterns with the stretch and recovery of L-PP fiber obtained at 1 km/min. Corresponding stress-strain behavior is also shown in the figure.

From Fig.8, it was found that the as-spun fiber obtained at 2 km/min was also consisting of monoclinic crystals. The major part of crystals showed c-axis orientation, whereas there was a co-existence of a certain amount of a*-axis oriented crystals. The SAXS pattern of as-spun fiber showed a fan-like two spot pattern, indicating the existence of highly oriented periodic structure of crystalline and amorphous phases. During the stretching, degree of orientation of c-axis oriented crystals decreased and the intensity of crystalline reflection corresponding to the a*-axis oriented crystals decreased in the WAXD patterns. In the SAXS patterns, two-spot patterns shifted to lower scattering angle, and its shape widened along the

horizontal direction. This result suggested the decrease of long period as well as the reduction of the size of periodic structure along the lateral direction. In the course of the recovery of fiber length to 19% stretch, WAXD and SAXS patterns virtually returned to the original patterns.

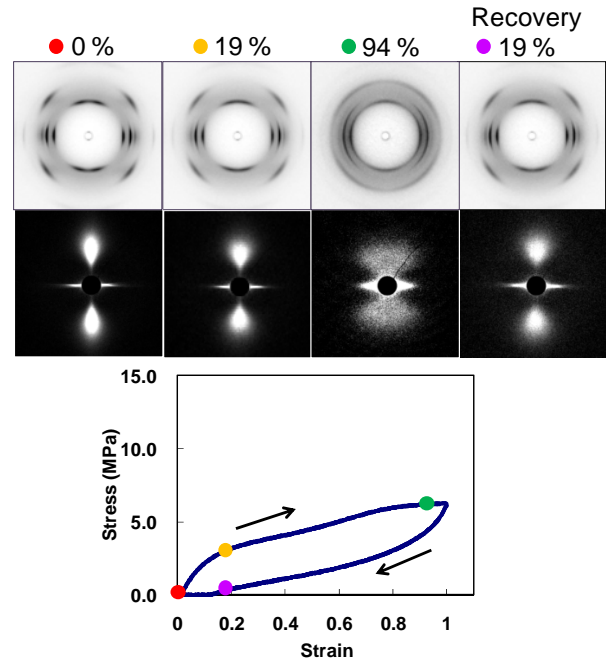


Fig.8 Changes of WAXD and SAXS patterns with the stretch and recovery of L-PP fiber obtained at 2 km/min. Corresponding stress-strain behavior is also shown in the figure.

It should be noted that the WAXD and SAXS patterns of L-PP-LMC fiber, which showed the maximum recoverability among the L-PP-LMC fibers obtained at different take-up velocities, also showed similar structural changes during stretch and recovery. In other words, good recoverability of higher-order structure after the stretching and recovery, which was characterized by the reduction of the amount of a*-axis oriented crystals and decrease of the orientation of c-axis oriented crystals during stretching, was found to be the characteristics of fibers with good elastic recoverability.

In case of the L-PP fiber obtained at 5 km/min (Fig.9), WAXD pattern indicated the structure of highly c-axis oriented monoclinic crystal with the only small amount of a*-axis oriented crystals. There was no distinct change of WAXD pattern during stretching as well as during recovery except for the slight increase and decrease of the intensities of crystalline reflections corresponding to the c-axis and a*-axis oriented crystals. SAXS pattern of the as-spun fiber showed the two-spot pattern with arc-shaped reflections on the meridian. The arc patterns gradually concentrated to the meridian with the stretching and reversibly returned to the original pattern after recovery.

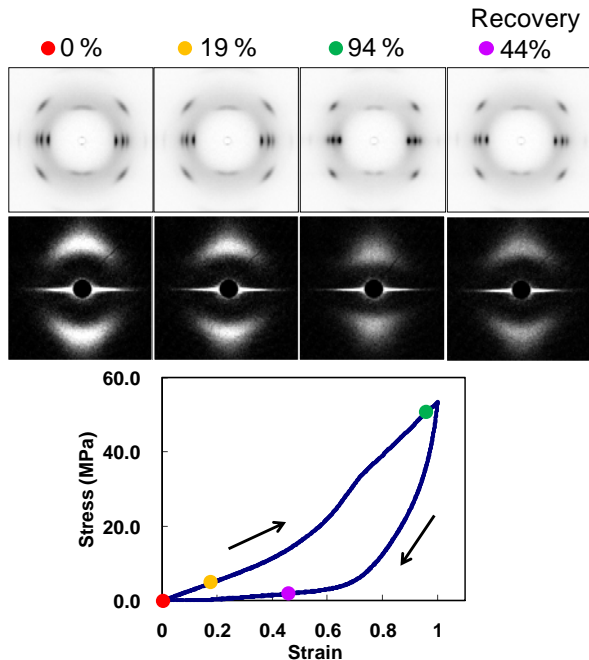


Fig.9 Changes of WAXD and SAXS patterns with the stretch and recovery of L-PP fiber obtained at 5 km/min. Corresponding stress-strain behavior is also shown in the figure.

Variation of long period with stretch and recovery was analyzed from the in-situ SAXS patterns. The results for L-PP 2 km/min fiber and L-PP-LMC 1 km/min fiber, both fiber showed good recoverability after stretching, are compared in Fig. 10. In both samples, variation of long period showed hysteresis during the first stretching and

recovery as in the case of stress-strain behavior. It should be noted that the ratio of the variation of long period with respect to the long period of original fiber is smaller than the stretch ratio of the fiber itself. Such discrepancy was more significant in case of L-PP fiber than the L-PP-LMC fiber. This is probably due to the difference in tensile stress appearing during the stretching of fibers. Nevertheless, it was concluded that the structure which was not reflected in the SAXS measurement exists in the fiber, and such structure also plays an important role for the elastic elongation of these fibers especially in case of L-PP.

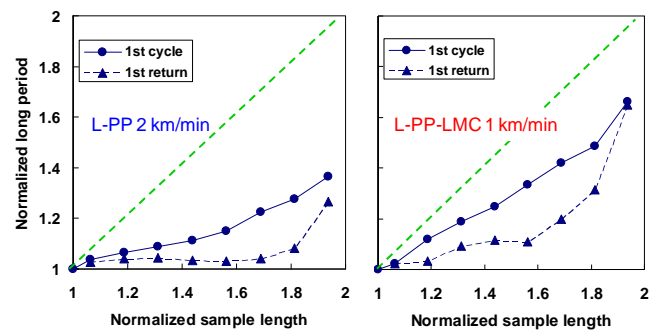


Fig.10 Variation of long period with stretching and recovery of L-PP 2 km/min fiber and L-PP-LMC 1 km/min fiber. Dotted line corresponds to the affine deformation of long period with respect to the elongation of fiber.

References

1. Shigeyuki Toki, Igors Sics, Chris Burger, Dufei Fang, Lizhi Liu, Benjamin S. Hsiao, Sudhin Datta, and Andy H. Tsou, *Macromolecules* **39**, 3588-3597 (2006)
2. Feng Zuo, Christian Burger, Xuming Chen, Yimin Mao, Benjamin S. Hsiao, Hongyu Chen, Gary R. Marchand, Shih-Yaw Lai, and Debbie Chiu : *Macromolecules* **43**, 1922–1929 (2010)
3. Y.Kohri, W.Takarada, H.Ito, T.Takebe, H.Minami, T.Kanai, T. Kikutani, *Seikei-kakou*, **20**, 11, 831-839 (2008)